Supplemental Material: Yang et al.

Figure S1. Anatomical characterization of NAcMed and NAcLat inputs to the VTA in A2a-Cre mice, Related to Figure 1.

(A) Schematic showing dual injection of AAVs expressing eYFP or mCherry into the NAcMed (medial shell of nucleus accumbens) and NAcLat (lateral shell of nucleus accumbens) of A2a-Cre mice, respectively.

(B) Fluorescence image showing eYFP-expression (green, 488 nm) in the NAcMed and mCherry-expression (red, 546 nm) in the NAcLat of a A2a-Cre mouse (blue: DAPI staining; aca: anterior commissure, CPu: caudate putamen, LS: lateral septum; Scale bar 50 μm).

(C) Fluorescence image of a coronal midbrain section showing TH-immunostaining (647 nm, blue) but absence of eYFP-expressing NAcMed terminals and mCherry-expressing NAcLat terminals (TH: tyrosine-hydroxylase, mVTA: medial VTA, lVTA: lateral VTA, IPN: interpeduncular nucleus, ml: medial lemniscus, SNc: substantia nigra pars compacta; Scale bar 50 μm).

Figure S2. Synaptic connectivity of NAc subnuclei with VTA DAergic and GABAergic subpopulations, Related to Figure 3.

(A) Sample confocal images from NAcLat terminal stimulation experiments in which individual retrogradely labeled neurons (546 nm, beads, red) were filled with neurobiotin (NB; 488 nm, green) via the recording pipette and immunostained for tyrosine-hydroxylase (TH; 647 nm, blue) (Scale bar 50 μm).

(B) Sample confocal images from NAcMed terminal stimulation experiments in which individual retrogradely labeled neurons (546 nm, beads, red) were filled with neurobiotin (NB; 488 nm, green) via the recording pipette and immunostained for tyrosine-hydroxylase (TH; 647 nm, blue) (Scale bar 50 μm).

(C) Schematic of AAV injection into the NAcMed or NAcLat of GAD2-tDTomato (GAD2-tdT) mice and *ex vivo* whole-cell patch-clamp recordings of tdTomato-expressing VTA neurons.

(D) Representative light-evoked inhibitory postsynaptic currents (IPSCs) recorded from tdTomato-expressing cells in the VTA for stimulation of NAcLat (upper trace) and NAcMed (lower trace) terminals in the VTA. The mean amplitude of light-evoked IPSCs recorded from GAD2-tdT-positive VTA neurons is significantly larger when stimulating NAcLat terminals in

the VTA compared to NAcMed terminal stimulation (* p = 0.0352) (Data represent means ± SEM).

(E) Sample confocal images from NAcMed (upper panel) and NAcLat (lower panel) terminal stimulation experiments in which individual GAD2-tdT-positive (546 nm, red) cells in the VTA were filled with neurobiotin (NB; 488 nm, green) via the recording pipette (Scale bar 50 µm).

(F) Bar graph showing that the percentage of GAD2-tDT-positive VTA cells responding to light stimulation is higher when the recording location in the VTA was matched with the respective NAc subregion. For example, the probability of recording light-evoked IPSCs was higher when NAcMed terminals were stimulated and the recorded cell was located in the mVTA, and lower when it was located in the lVTA. The opposite applies for NAcLat terminal stimulation.

(G) Schematic showing dual injection of AAVs expressing eYFP into the NAcMed and mCherry into the VTA of GAD2-Cre mice, respectively (upper left panel). Fluorescence image showing eYFP-expression (green, 488 nm) in the NAcMed of a GAD2-Cre mouse (blue: DAPI staining; lower left panel). Confocal images of coronal midbrain sections showing TH-immunostaining (647 nm, blue) in the lateral VTA (lVTA, middle panel) and medial VTA (mVTA, right panel). Note that eYFP-expressing NAcMed terminals are located in close proximity of mCherry-positive cells (i.e., GABAergic neurons; white arrow heads) in the mVTA but not lVTA (Scale bar 50 µm).

(H) Same approach as in (G), but for injection of AAVs expressing eYFP into the NAcLat and mCherry into the VTA of GAD2-Cre mice. Note that eYFP-expressing NAcLat terminals are located in close proximity of mCherry-positive cells (i.e., GABAergic neurons; white arrow heads) in the lVTA but not mVTA (Scale bar 50 µm).

(I) Schematic showing dual injection of red retrobeads into the NAcMed and NAcLat, AAV injection into the VTA and *ex vivo* whole-cell patch-clamp recordings of retrogradely labeled NAcMed- and NAcLat-projecting VTA DA neurons in GAD2-Cre mice.

(J) Representative light-evoked IPSCs recorded from a NAcLat-projecting DA neuron (upper trace) and NAcMed-projecting DA neuron (lower trace) in response to light stimulation of GABAergic terminals in the VTA. Light-evoked IPSCs were blocked by bath application of 50 µM picrotoxin (PCTX, red traces). The mean amplitude of light-evoked IPSCs recorded from NAcLat-projecting DA neurons is significantly larger compared to NAcMed-projecting DA neurons (*** p = 0.0005) (Data represent means ± SEM).

Figure S3. Complete serial reconstructions of AAV injection sites and optical fiber placements for behavioral experiments shown in Figures 4 and 5.

(A) Schematic drawings showing rostro-caudal distribution for ChR2-eYFP expression of mice injected with AAVs into the NAcMed (solid lines) or NAcLat (dashed lines) as well as corresponding optical fiber placements in the midbrain (solid lines for mice injected with AAVs into NAcMed and dashed lines for mice injected with AAVs into NAcLat). Different colors are used to outline the brains regions in which ChR2-EYFP was detected as well as for the placements of the optical fiber with each color representing the expression profile and fiber placement from a single animal.

(B) Representative fluorescence images showing ChR2-eYFP expression (488 nm, green) of mice injected with AAV-DIO-ChR2-eYFP in the NAcMed along the rostro-caudal axis of the ventral striatum (blue: DAPI staining) (Scale bar 100 μm).

(C) Same as in (B) but for mice injected with AAV-DIO-ChR2-eYFP into NAcLat (Scale bar 100 μm).

Figure S4. Assessment of locomotor behavior in response to *in vivo* optogenetic stimulation of NAcLat and NAcMed terminals in the VTA, Related to Figures 4 and 5.

(A) Schematic of open field test, which involves 20 Hz light stimulation of NAcLat terminals in the VTA of D1-Cre mice during a 3-min light-on epoch (upper left panel). Representative trajectory of an animal during the initial 3-min light-off epoch (lower left panel), during the 3-min light-on epoch (upper right panel) and final 3-min light-off epoch (lower right panel). The bar graphs show that light stimulation of NAcLat terminals in the VTA did not significantly alter track length (left; off: 374.1 ± 61.27 cm, on: 542.7 ± 79.11 cm, off: 237.7 ± 45.18 cm, n = 9, RM one-way ANOVA, $p_{off\ vs.\ on} = 0.2881$, $p_{off\ vs.\ off} = 0.0565$, $p_{on\ vs.\ off} = 0.0675$), velocity (middle; off: 2.08 ± 0.34 cm/s, on: 3.01 ± 0.44 cm/s, off: 1.32 ± 0.25 cm/s, n = 9; RM one-way ANOVA, $p_{off\ vs.\ on} = 0.302$, $p_{off\ vs.\ off} = 0.0546$, $p_{on\ vs.\ off} = 0.0702$) and time spent in center (right; off: 3.62 ± 1.37 s, on: 4.44 ± 1.29, off: 7.28 ± 3.44, n = 9; RM one-way ANOVA, $p_{off\ vs.\ on} = 0.6876$, $p_{off\ vs.\ off} = 0.3717$, $p_{on\ vs.\ off} = 0.5364$) (Data represent means ± SEM).

(B) Same approach as in (A) but for light stimulation of NAcMed terminals. Note that stimulation of NAcMed terminals significantly reduced track length (left; off: 675.5 ± 155.7 cm, on: 903.4 ± 133.9 cm, off: 210.1 ± 80.99 cm, n = 10, RM one-way ANOVA, $p_{off\ vs.\ on} = 0.263$, ** $p_{off\ vs.\ off} = 0.0031$, *** $p_{on\ vs.\ off} = 0.0006$) and velocity (middle; off: 3.76 ± 0.87 cm/s, on: 5.02 ±

0.74 cm/s, off: 1.17 ± 0.45 cm/s, n = 10; RM one-way ANOVA, $p_{off\ vs.\ on} = 0.2646$, ** $p_{off\ vs.\ off} = 0.003$, *** $p_{on\ vs.\ off} = 0.0005$) in the last 3-min light-off epoch. However, no significant changes were observed in time spent in center area (right; off: 3.82 ± 0.85 s, on: 9.25 ± 2.45, off: 5.31 ± 2.14, n = 10; RM one-way ANOVA, $p_{off\ vs.\ on} = 0.1505$, $p_{off\ vs.\ off} = 0.8191$, $p_{on\ vs.\ off} = 0.0614$) (Data represent means ± SEM).

Figure S5. Optogenetic silencing of NAcLat terminals in the VTA, Related to Figure 4.
(A) Schematic of AAV injection into the NAcLat of D1-Cre mice and inhibition of NAcLat terminals in the VTA.
(B) Schematic of real-time place preference assay, which involves switching of light stimulated compartments after 10 min.
(C) Trajectory of a mouse that received terminal inhibition in one compartment (top panel) for the initial 10 min period and then received terminal inhibition in the other compartment (lower panel) for an additional 10 min.
(D) Bar graph showing that inhibition of NAcLat terminals does not significantly alter place preference behavior (non-stim.: 560.4 ± 31.16 s, stim.: 483.4 ± 47.64 s, n = 6; p = 0.3376) (Data represent means ± SEM).
(E) Bar graph showing that inhibition of NAcLat terminals does not significantly alter number of compartment entries (non-stim.: 17.17 ± 4.6, stim.: 13.67 ± 2.91, n = 6; p = 0.121) (Data represent means ± SEM).

Figure S6. Analysis of $GABA_B$ receptor transmission in VGLUT2-expressing VTA cell populations, Related to Figure 6.
(A) Schematic showing AAV injection into the lateral VTA (lVTA) and green retrobead injection into the NAcLat of VGLUT2-Cre mice to investigate VGLUT2 expression in NAcLat-projecting DA neurons.
(B) Confocal images showing VGLUT2-expressing (mCherry-positive, red) neurons in the caudal midbrain at low (left, scale bar 200 μm) and high (right, scale bar 10 μm) magnification. Most NAcLat-projecting (beads, green) DA (TH-positive, blue) neurons do not co-express VGLUT2.
(C-D) Same as in (A-B) but for AAV injection into the medial VTA (mVTA) and green retrobead injection into the NAcMed. Most NAcMed-projecting DA neurons co-express

VGLUT2.

(E) Summary of VGLUT2-expression analysis for NAcMed- and NAcLat-projecting DA neurons (NAcMed: n = 162 cells (from n = 3 mice), mCherry+ TH+ = 58.02%, mCherry+ TH- = 5.56%, mCherry- TH+ = 33.95%, mCherry+ TH- = 2.47%; NAcLat: n = 180 cells (from n = 4 mice), mCherry+ TH+ = 15.56%, mCherry+ TH- = 5%, mCherry– TH+ = 77.22%, mCherry- TH- = 2.22%, Chi-square (71.33), *** $p < 0.0001$).

(F) Confocal images of the rostral midbrain in low (left, scale bar 100 μm) and high (right, scale bar 10 μm) magnification showing a large number of VGLUT2-positive, TH-negative cells in the rostral VTA (rVTA).

(G) Schematic showing AAV injection into the VTA of VGLUT2-Cre mice and *ex vivo* whole-cell patch-clamp recordings of mCherry (i.e., VGLUT2)-expressing VTA neurons.

(H) Outward currents (recorded at -55 mV, in 50 μM picrotoxin, 20 μM CNQX, 50 μM D-AP5) are plotted as a function of time for VGLUT2+ TH- (white circles) and VGLUT2+ TH+ (grey circles) VTA neurons. Bath application of 100 μM baclofen induces a small outward current in both populations, which is comparable to the current observed in NAcMed-projecting DA neurons (Figure 6B) (Data represent means ± SEM).

(I) Bar graph showing no significant difference in peak outward currents evoked by baclofen between VGLUT2+ TH- and VGLUT2+ TH+ VTA neurons (VGLUT2+ TH- 35.03 ± 12.36 pA, n = 9; VGLUT2+ TH+ 23.38 ± 8.14 pA, n = 8; $p = 0.4558$) (Data represent means ± SEM).

(J) Anatomical locations of all recorded neurons. Note, that most VGLUT2+ TH+ neurons are located in the mVTA of the caudal midbrain, while VGLUT2- TH- neurons are mainly located in the rostral midbrain.

(K) Sample confocal images for recordings from VGLUT2-expressing (mCherry-positive, red) and neurobiotin-filled cells (NB, green) that are TH-immunonegative (upper row) or TH-immunopositive (blue, lower row) (Scale bar 50 μm).

Figure S7. Optogenetic stimulation of NAcLat terminals in the VTA does not elicit $GABA_B$ receptor-mediated currents in NAcLat- and NAcMed-projecting DA neurons, Related to Figure 6.

(A) Schematic of AAV injection into NAcLat and red retrobead injection into NAcMed and NAcLat of D1-Cre mice. Whole-cell patch clamp recordings were performed from retrogradely labeled neurons in different VTA subregions while stimulating NAcLat terminals in the VTA.

(B) No detectable outward currents in response to 20 Hz light stimulation of NAcLat terminals in NAcLat- (upper panel, n = 7 cells) and NAcMed-projecting (lower panel, n = 3 cells) DA neurons (cells held at −55 mV; recorded in 50 µM picrotoxin, 20 µM CNQX, 50 µM D-AP5).
(C) Left: Sample whole-cell patch clamp recordings of spontaneous firing from a NAcLat-projecting DA neuron and 20 Hz light stimulation of NAcLat terminals before (black trace) and after (red trace) bath application of 100 µM CGP35348. Right: Bar graph showing the mean firing frequency of NAcLat-projecting DA neurons before (off, white bar) and during 20 Hz light stimulation (blue bars) of NAcLat terminals in the VTA (off: 0.51 ± 0.14 Hz; ACSF: 1.81 ± 0.41 Hz; CGP: 1.76 ± 0.42 Hz, n = 9; RM one-way ANOVA, * $p_{off\ vs.\ ACSF} = 0.0276$, * $p_{off\ vs.\ CGP} = 0.0435$, $p_{ACSF\ vs.\ CGP} = 0.6627$) (Data represent means ± SEM).
(D) Same as in (C), but recordings were performed from NAcMed-projecting DA neurons (off: 3.6 ± 0.71 Hz; ACSF: 3.74 ± 0.65 Hz; CGP: 2.29 ± 0.35 Hz, n = 14; RM one-way ANOVA, $p_{off\ vs.\ ACSF} = 0.5225$, $p_{off\ vs.\ CGP} = 0.1285$, $p_{ACSF\ vs.\ CGP} = 0.0511$) (Data represent means ± SEM).

Figure S8. Complete serial reconstructions of AAV injection sites and placements of the optofluidic system for behavioral experiments shown in Figure 7.
Left panels show representative fluorescence images of ChR2-eYFP expression (488 nm, green) in the NAcMed (A, Scale bar 50 µm) and a coronal midbrain section showing TH-immunofluorescence (red, 546 nm), ChR2-eYFP expressing NAcMed terminals as well as optofluidic system placement (B, Scale bar 100 µm). Right panels show schematic drawings of the rostro-caudal distribution for ChR2-eYFP expression of mice injected with AAVs into the NAcMed (A) and corresponding optofluidic system placements in the ventral midbrain (B). Different colors are used to outline the brains regions in which ChR2-eYFP was detected and for the placements of the optofluidic system with each color representing the expression profile and placement from a single animal (RLi: rostral linear nucleus, SNr: substantia nigra pars reticulata, ml: medial lemniscus, PAG: periaqueductal gray, MS: medial septum, LV: lateral ventricle)

Suppl. Fig.1 Yang et al.

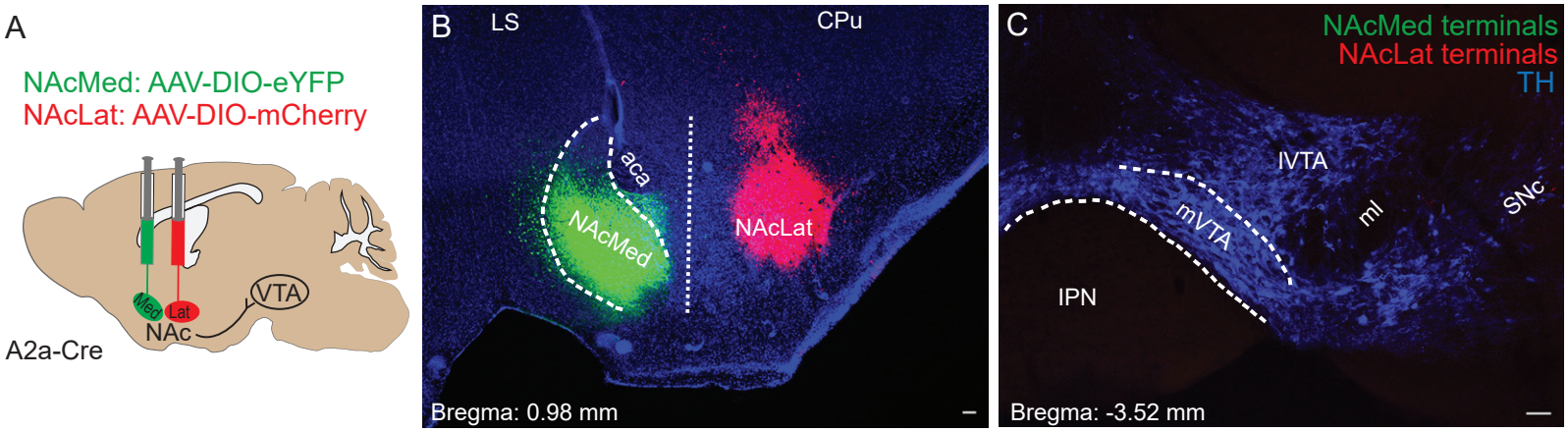

Suppl. Fig.2 Yang et al.

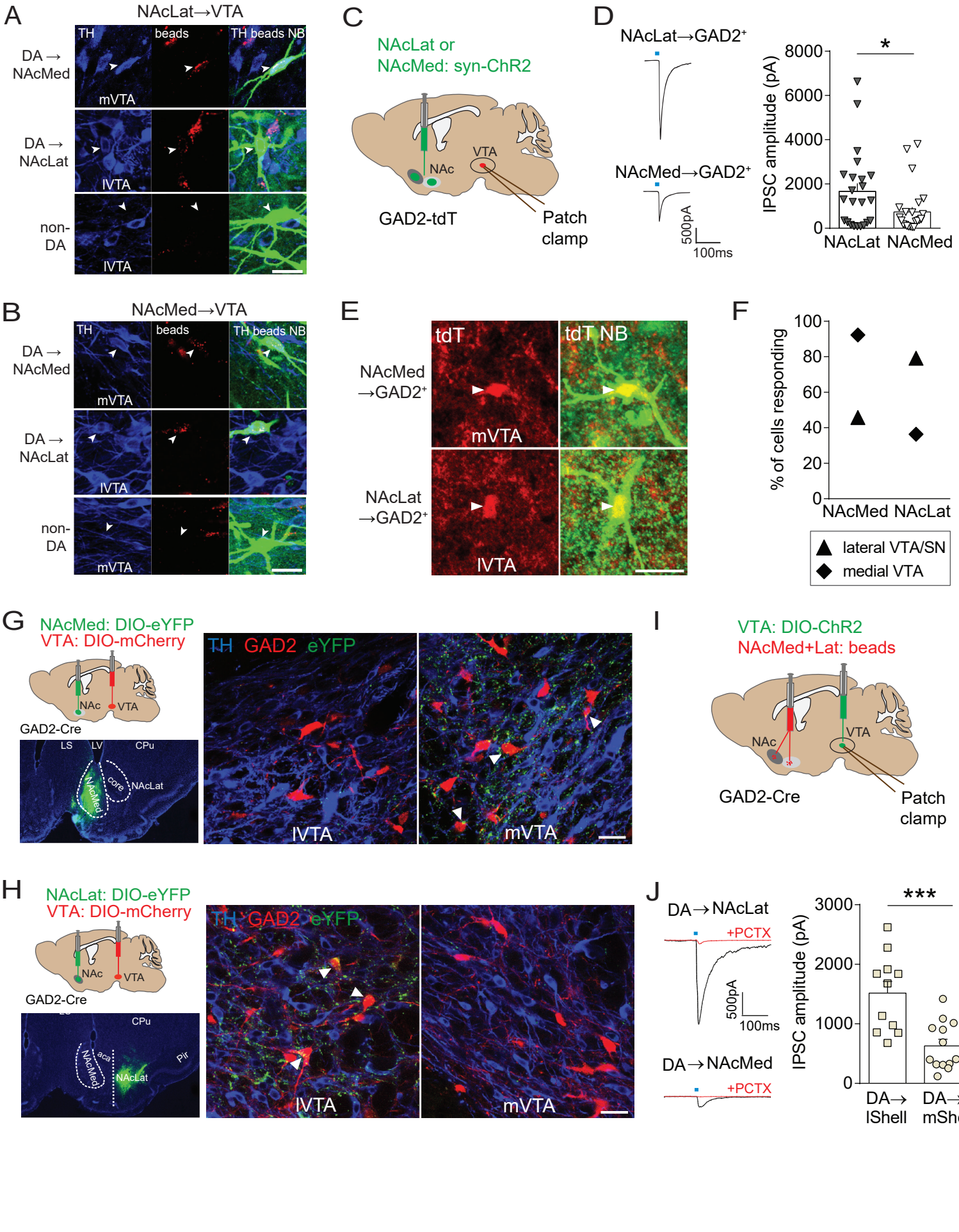

Suppl. Fig.3 Yang et al.

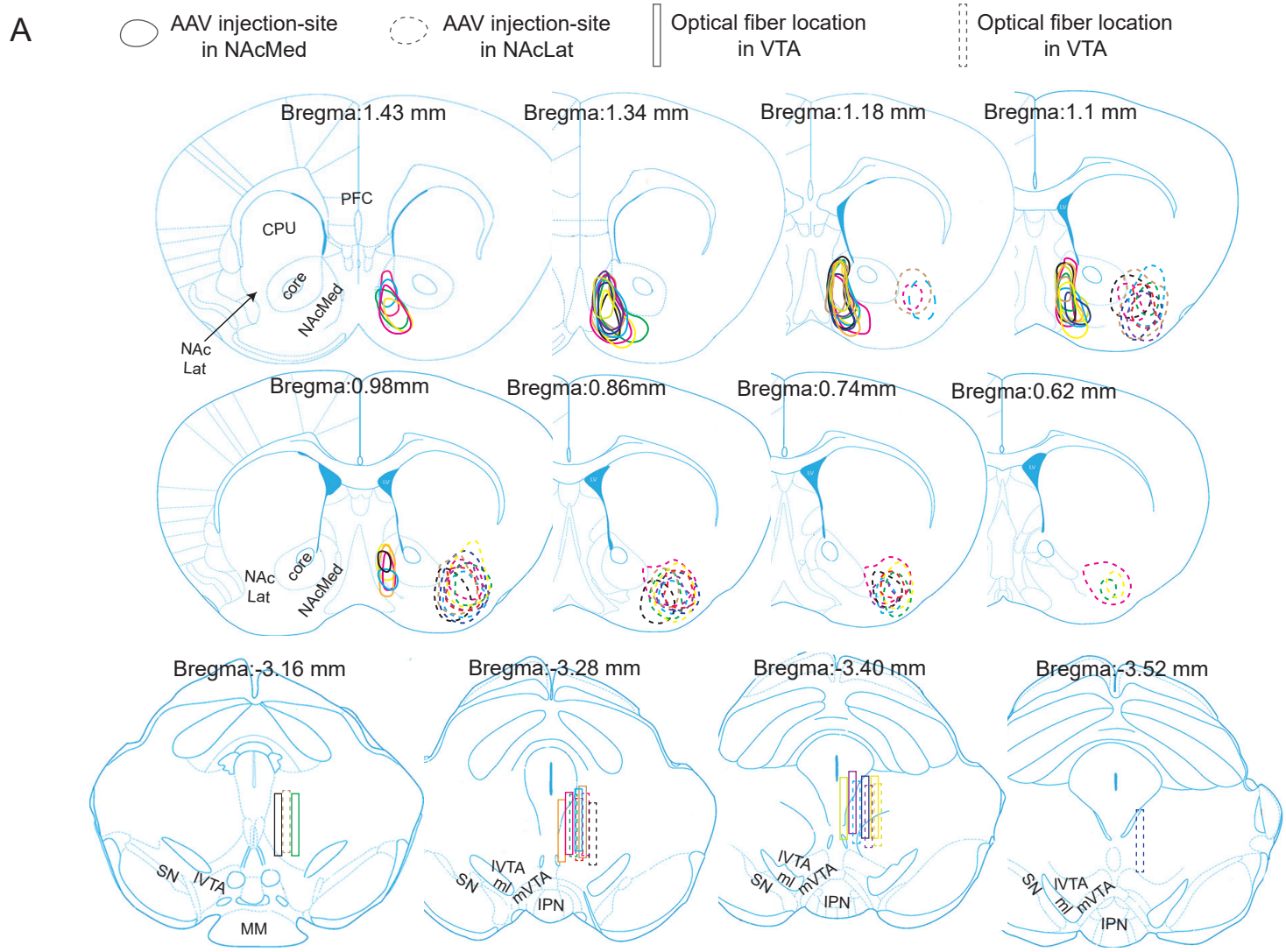

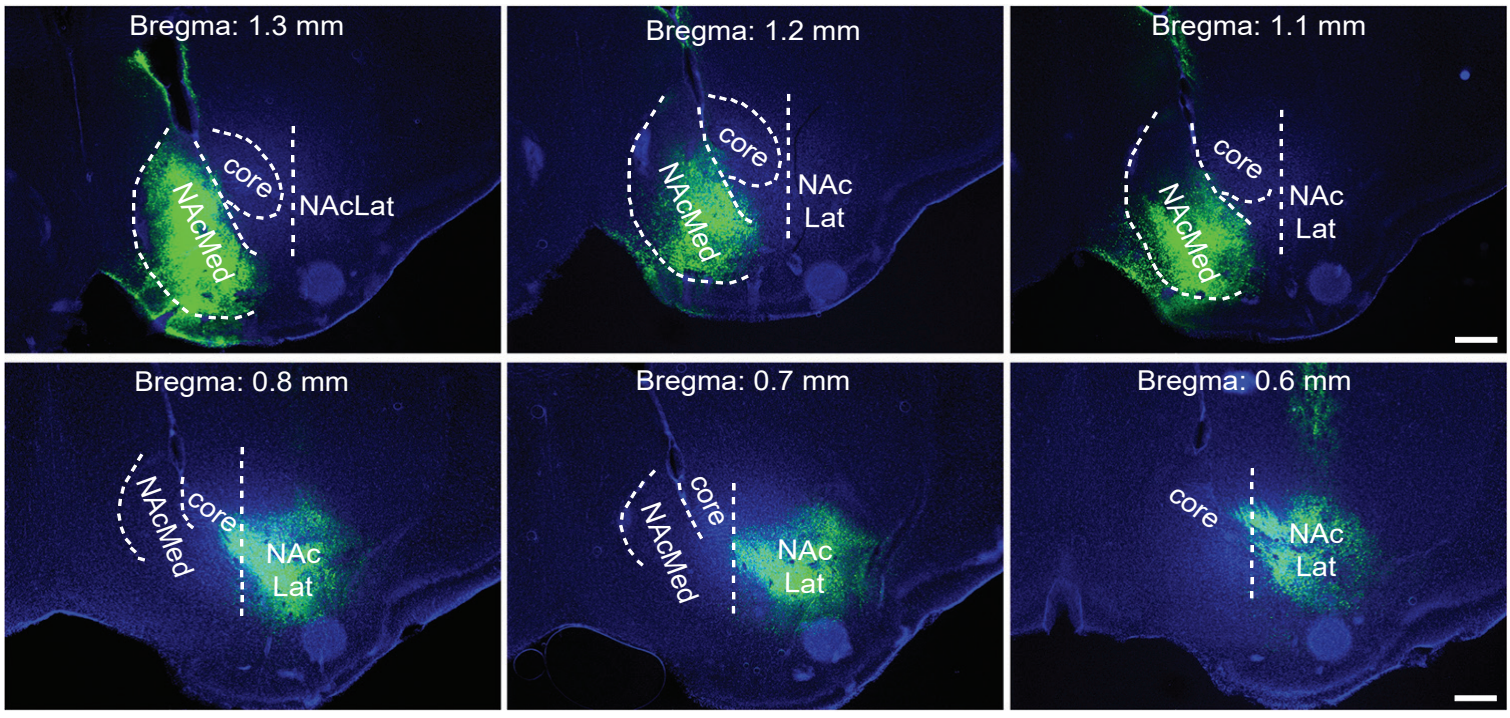

Suppl. Fig.4 Yang et al.

A

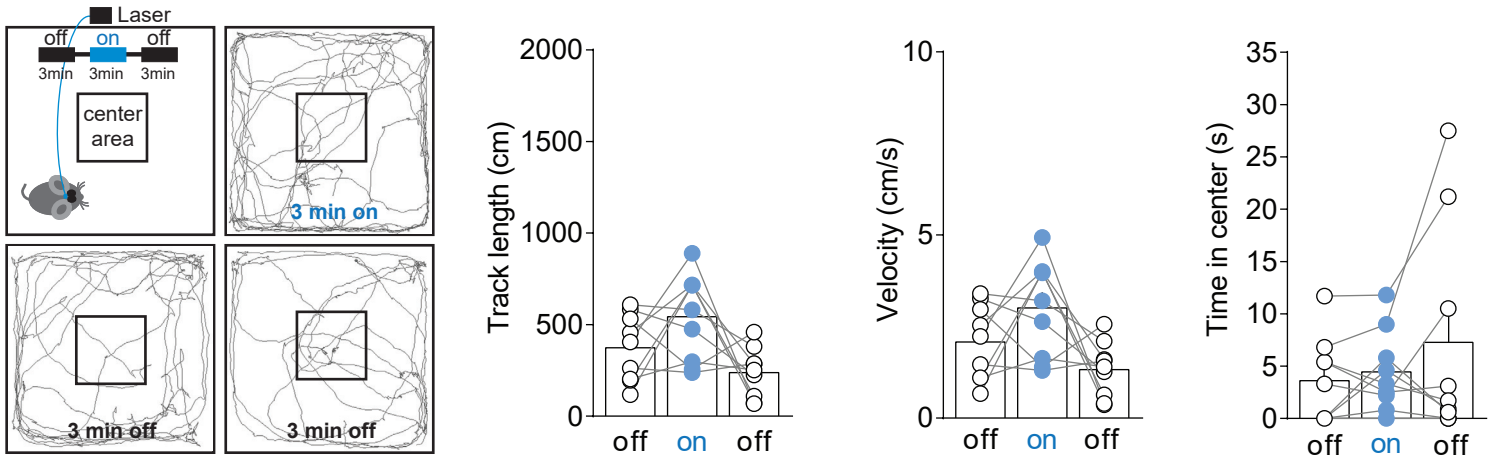

B

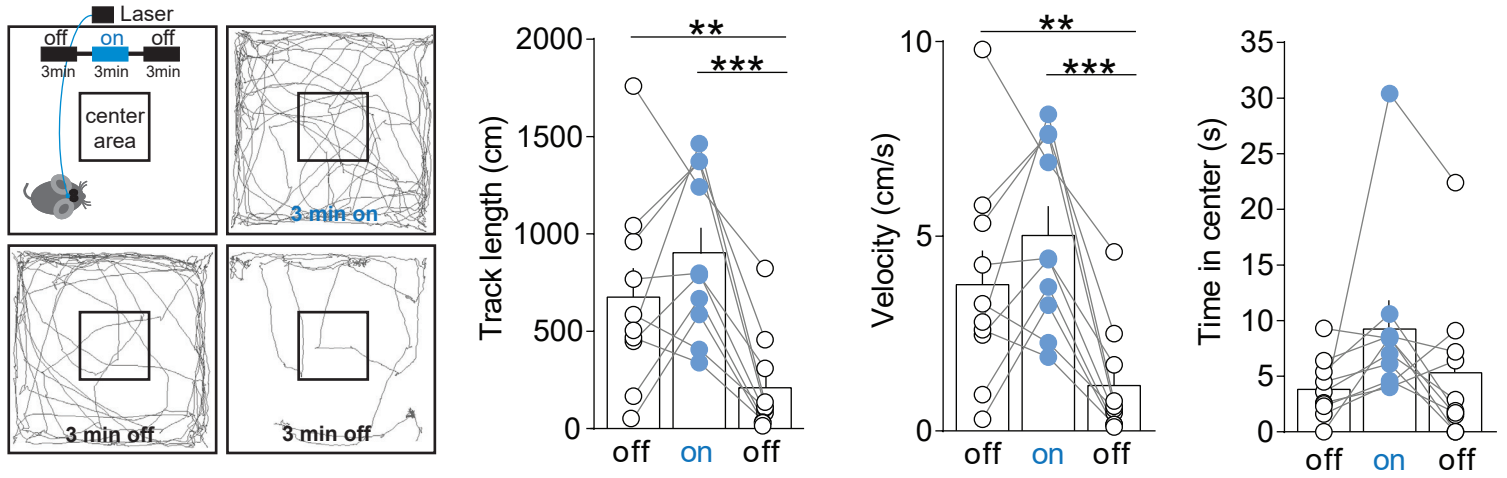

Suppl. Fig.5 Yang et al.

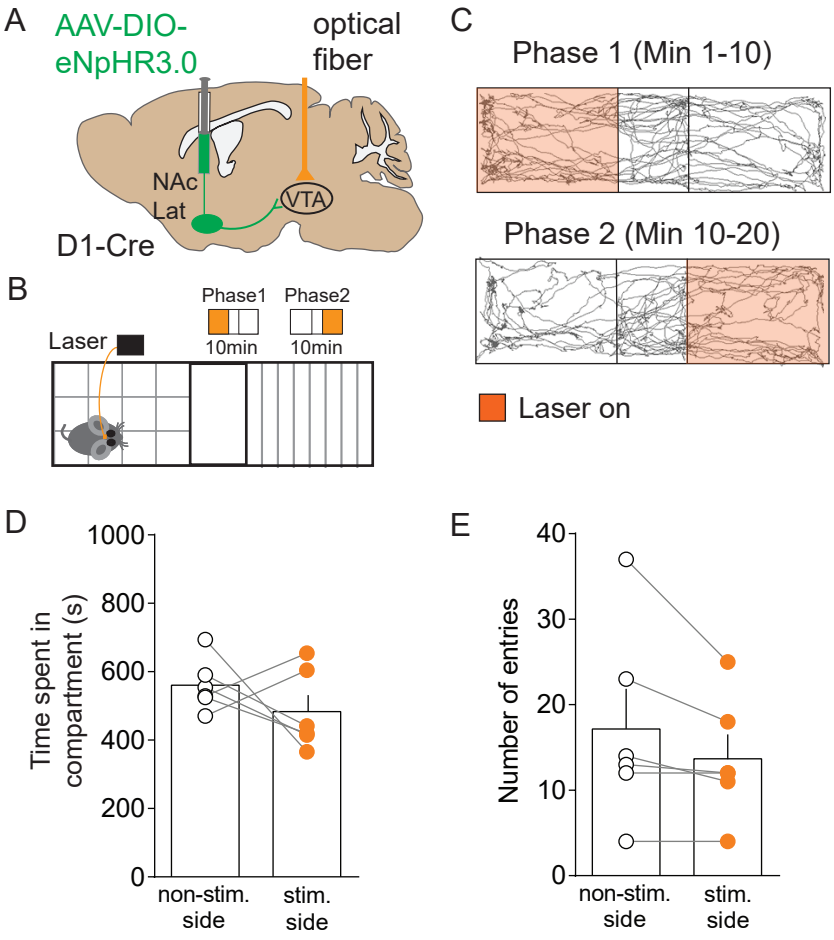

Suppl. Fig.6 Yang et al.

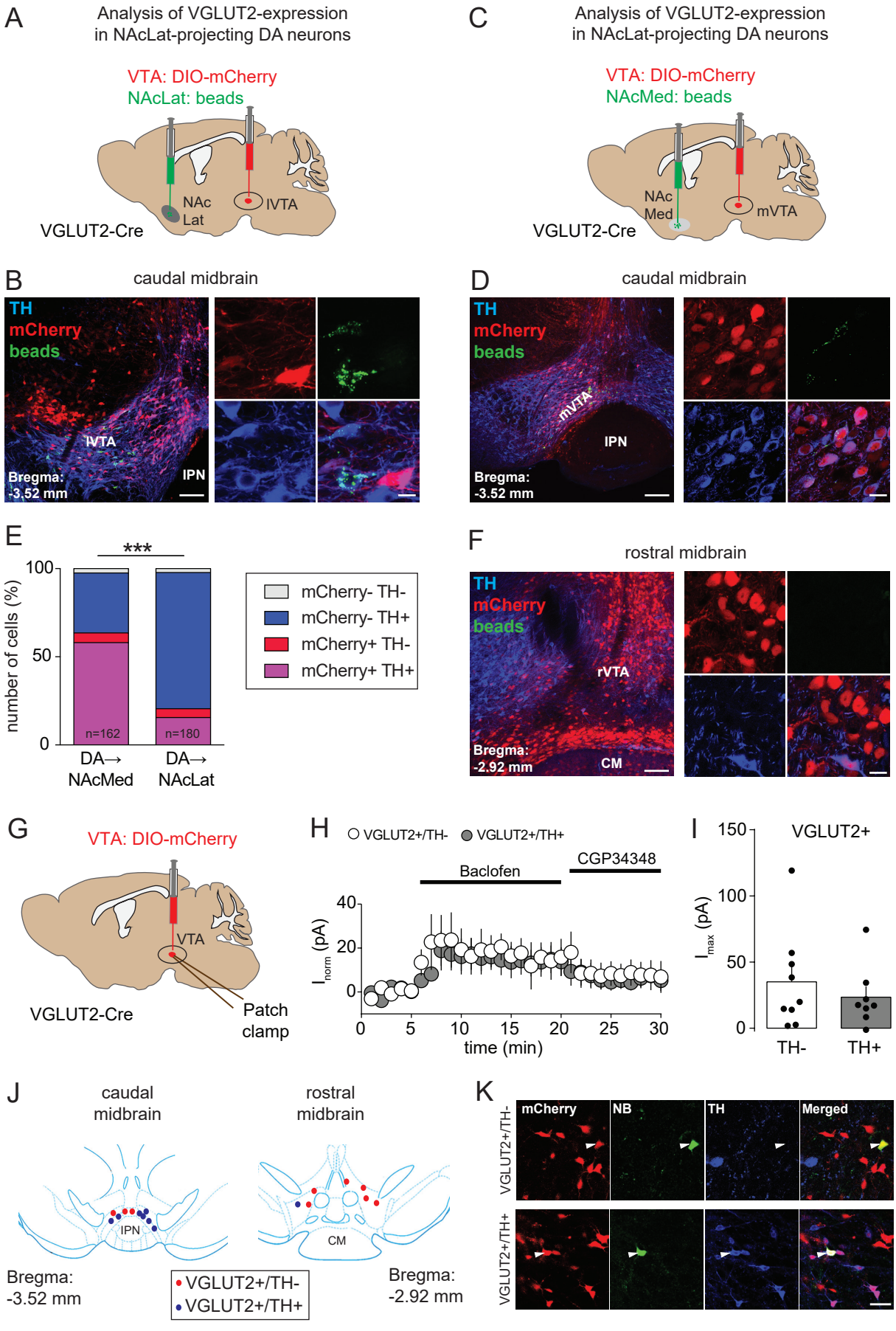

Suppl. Fig.7 Yang et al.

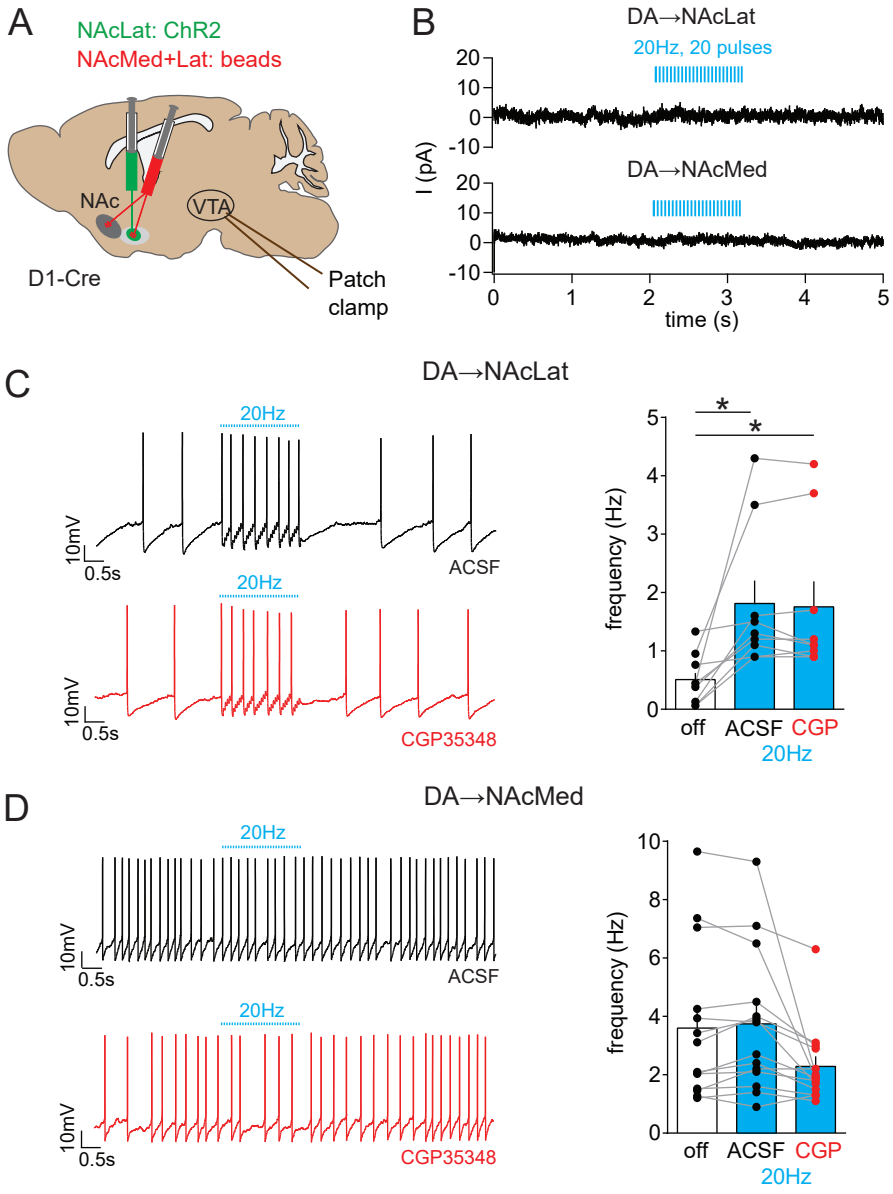

Suppl. Fig.8 Yang et al.

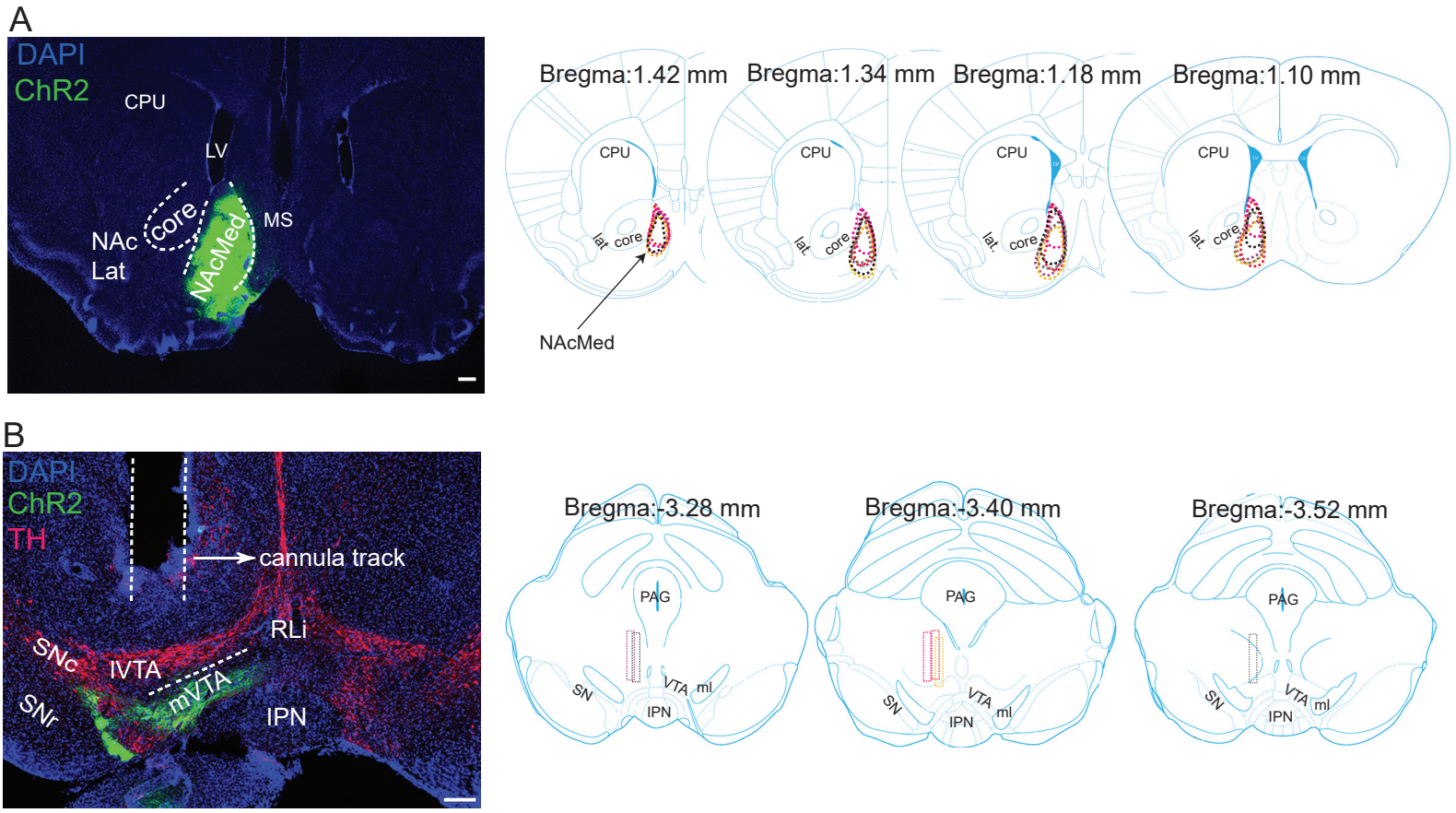

Table S1. Summary of statistical analysis

Data:	Statistical Test:	n	outcome measure	p value
Figure 1E	Unpaired t-test	NAcMed: 3 mice; average of 4 images for each mice NAcLat: 3 mice; average of 4 images for each mice	Fluorescence (%)	NAcMed->mVTA vs NAcMed->lVTA: 0.0026 NAcLat->mVTA vs NAcLat->lVTA: 0.0237
Figure 2E	Unpaired t-test	8 cells from 3 mice	mIPSCs amplitude	0.4414
Figure 2F	Unpaired t-test	8 cells from 3 mice	Firing frequency	<0.0001
Figure 3B	Unpaired t-test	7 cells (DA->NAcMed) 24 cells (DA->NAcLat) from 4 mice	IPSC amplitude	0.5879
Figure 3C	Paired t-test	10 cells from 4 mice	IPSC amplitude	0.0173
Figure 3D	Unpaired t-test	13 cells (DA->NAcLat) 5 cells (non DA) from 3 mice	IPSC amplitude	0.0007
Figure 3F	One-way repeated measures ANOVA with Tukey's post hoc test.	20 cells from 7 mice	Firing frequency	Effect of stimulation: 0.0001 Post hoc: off vs on: 0.0002 off vs off: 0.5163 on vs off: 0.0004
Figure 3H	Unpaired t-test	15 cells (DA->NAcMed) 7 cells (DA->NAcLat) from 5 mice.	IPSC amplitude	0.018
Figure 3I	Paired t-test	6 cells from 5 mice	IPSC amplitude	0.0129
Figure 3J	Unpaired t-test	10 cells (DA->NAcMed) 7 cells (non DA) from 3 mice	IPSC amplitude	0.161
Figure 3L	One-way repeated measures ANOVA with Tukey's post hoc test.	17 cells from 6 mice	Firing frequency	Effect of stimulation: 0.0079 Post hoc: off vs on: 0.0258 off vs off: 0.9054 on vs off: 0.0298
Figure 4F	Paired t-test	9 mice	Time spent in compartment	0.0001
Figure 4G	Paired t-test	9 mice	Number of entries	0.0038
Figure 4H	Unpaired t-test	9 mice (ChR2) 6 mice (eYFP)	Nosepokes	0.0021
Figure 4I	One-way repeated measures ANOVA with Tukey's post hoc test.	8 mice	Time spent in open arms	Effect of stimulation: 0.2618 Post hoc: off1 vs 20hz: 0.2473 20hz vs off2: 0.9662 off1 vs off2: 0.2688
Figure 5F	Paired t-test	10 mice	Time spent in compartment	0.6897
Figure 5G	Unpaired t-test	10 mice (ChR2) 6 mice (eYFP)	Nosepokes	0.184
Figure 5H	Two-way ANOVA with Holm-Sidak's post hoc test	10 mice (NAcMed ChR2) 6 mice (NAcMed eYFP) 9 mice (NAcLat ChR2) 8 mice (NAcLat eYFP)	Time spent in neutral area's.	Effect of projection: 0.0004 Effect of ChR2: 0.9441 Interaction: 0.0002 Post hoc: NAcMed->mVTA vs NAcMed->lVTA: 0.0097
Figure 5I	One-way repeated measures ANOVA with Tukey's post hoc test.	10 mice	Time spent in open arms.	Effect of stimulation: 0.0146 Post hoc: off vs on: 0.9191 off vs off: 0.0664 on vs off: 0.0484
Figure 6C	Unpaired t-test	7 cells (DA->NAcLat) 6 cells (DA->NAcMed) from 3 mice	Maximum current	0.0024
Figure 6F	Unpaired t-test	18 cells (ACSF) 8 cell (CGP) from 6 mice	GABA-B current	0.0028
Figure 6G	One-way repeated measures ANOVA with Tukey's post hoc test.	7 cells from 5 mice	Firing frequency	Main effect: 0.0007 Post hoc: off vs ACSF: 0.0066 off vs CGP: 0.4306 ACSF vs CGP: 0.0081
Figure 6H	One-way repeated measures ANOVA with Tukey's post hoc test.	10 cells from 4 mice	Firing frequency	Main effect: < 0.0001 Post hoc: off vs ACSF: 0.0004 off vs CGP: 0.0004 ACSF vs CGP: 0.994
Figure 7C	Paired t-test	6 mice	Time spent in compartment	0.4353

Figure 7D	Paired t-test	6 mice	Time spent in compartment	<0.0001
Figure 7E	One-way repeated measures ANOVA with Tueky's post hoc test.	6 mice	Time spent in open arms.	Effect of stimulation: 0.0024 Post hoc: off vs on: 0.9996 off vs off: 0.0203 on vs off: 0.0219
Figure 7F	One-way repeated measures ANOVA with Tueky's post hoc test.	6 mice	Time spent in open arms.	Effect of stimulation: 0.2469 Post hoc: off vs on: 0.4417 off vs off: 0.5688 on vs off: 0.435
Figure S2D	Unpaired t-test	23 cells (NAcLat) 23 cells (NAcMed) from 3 mice	IPSC amplitude	0.0352
Figure S2J	Unpaired t-test	11 cells (DA->NAcLat) 13 cells (DA->NAcMed) from 5 mice	IPSC ampliude	0.0005
Figure S4A panel 1	One-way repeated measures ANOVA with Tukey's post hoc test.	9 mice	Track length	Effect of stimulation: 0.364 Post hoc: off vs on: 0.2881 off vs off: 0.0565 on vs off: 0.0675
Figure S4A panel 2	One-way repeated measures ANOVA with Tukey's post hoc test.	9 mice	Velocity	Effect of stimulation: 0.0386 Post hoc: off vs on: 0.302 off vs off: 0.0546 on vs off: 0.0702
Figure S4A panel 3	One-way repeated measures ANOVA with Tukey's post hoc test.	9 mice	Time in center	Effect of stimulation: 0.2456 Post hoc: off vs on: 0.6876 off vs off: 0.3717 on vs off: 0.5364
Figure S4B panel 1	One-way repeated measures ANOVA with Tukey's post hoc test.	10 mice	Track length	Effect of stimulation: 0.0001 Post hoc: off vs on: 0.263 off vs off: 0.0031 on vs off: 0.0006
Figure S4B panel 2	One-way repeated measures ANOVA with Tukey's post hoc test.	10 mice	Velocity	Effect of stimulation: 0.0001 Post hoc: off vs on: 0.2646 off vs off: 0.003 on vs off: 0.0005
Figure S4B panel 3	One-way repeated measures ANOVA with Tukey's post hoc test.	10 mice	Time in center	Effect of stimulation: 0.0862 Post hoc: off vs on: 0.1505 off vs off: 0.8191 on vs off: 0.0614
Figure S5D	Paired t-test	6 mice	Time spent in compartment	0.3376
Figure S5E	Paired t-test	6 mice	Number of entries	0.121
Figure S6E	Chi-square test	NAcMed: 162 cells from 3 mice NAcLat: 180 cells from 4 mice	Number of cells	<0.0001
Figure S6I	Unpaired t-test	9 cells (TH-) 8 cells (TH+) from 4 mice	Maximum Current	0.4558
Figure S7C	One-way repeated measures ANOVA with Tukey's post hoc test.	9 cells form 5 mice	Firing frequency	Main effect: 0.014 Post hoc: off vs ACSF: 0.0276 off vs CGP: 0.0435 ACSF vs CGP: 0.6627
Figure S7D	One-way repeated measures ANOVA with Tukey's post hoc test.	14 cells from 4 mice	Firing frequency	Main effect: 0.0348 Post hoc: off vs ACSF: 0.5225 off vs CGP: 0.1285 ACSF vs CGP: 0.0511